Micromachining using femtosecond laser pulses

1. Overview of femtosecond laser pulses
   - some acronyms
   - laser system
   - diagnostic tools
   - properties
2. Micromachining
   - modeling
   - short pulse (<ps) vs. long pulse (>ps)
   - animations
   - micromachining on dielectric
   - some results
3. Conclusions

1 femtosecond (fs) $= 10^{-15}$ second $= 0.3$ μm in vacuum
1 attosecond (as) $= 10^{-18}$ second $= 0.3$ nm in vacuum

Transform – limited – pulse

$$\Delta t \, \Delta E = h$$

$$\Delta t \text{ (fs)} \, \Delta\lambda \text{ (nm)} = \frac{4.4 \text{x} 10^3}{3} \lambda^2 \text{ } (\mu\text{m}) \qquad \text{Gaussian pulse}$$

λ (nm)	E (eV)	Δt (fs)	$\Delta\lambda$ (nm)	$\Delta\nu$ (GHz)
800	1.55	100	9.4	4400
800	1.55	17	55	26,000
800	1.55	4	235	110,000
13.7	90	$\sim$0.65	-	-

* one optical cycle = 2.67 fs at 800 nm

Ti:sapphire laser oscillator

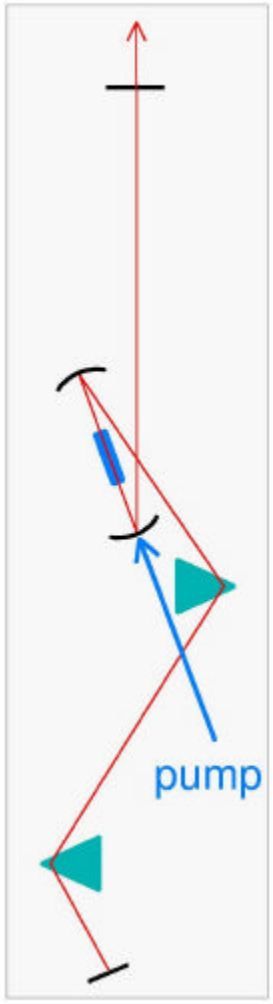

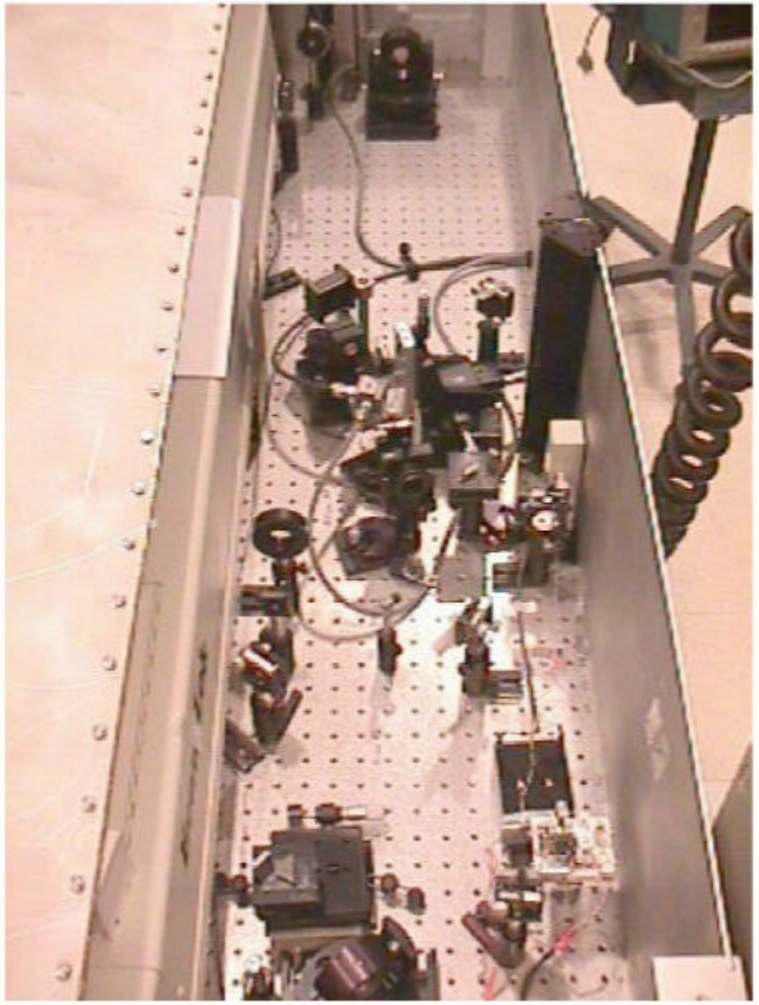

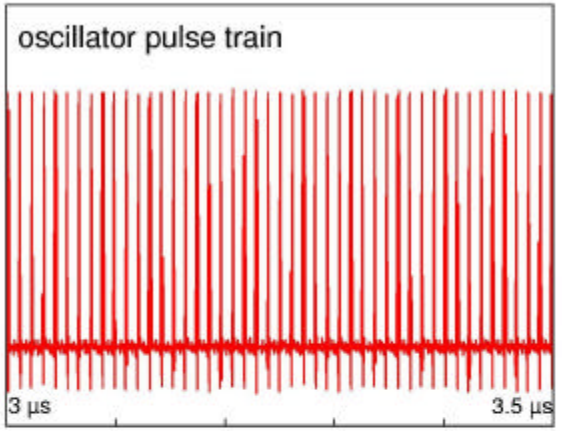

100 MHz repetition rate

100 fs

800 nm (1.55 eV)

3 nJ/pulse (10^{10} photons)

30 kW/pulse

5×10^{12} Watts/cm^2

Combined SPM and dispersion compensation - short pulse formation

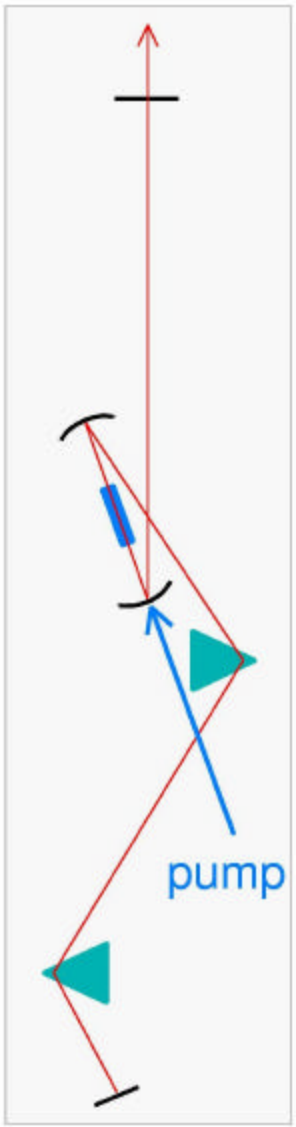

Self-phase modulation - nonlinear effect

$n(t) = n_o + n_2[I(t)]$

$\Delta\omega \sim \Delta\theta(t) \sim \Delta n(t) \sim n_2[I(t)]$

spectral profile

temporal profile

glass or laser crystal

Prism pair (dispersion compensation)

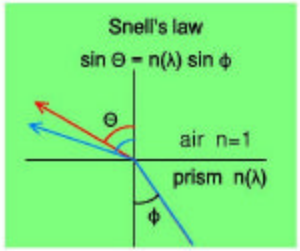

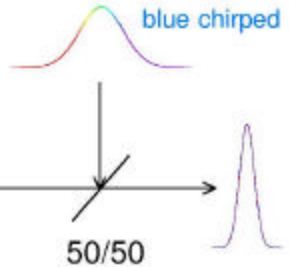

$$T(\omega) = \frac{d\phi}{d\omega} = T_0 = \text{constant}$$

$$\phi(\omega) = \phi_o + \phi_1(\omega - \omega_o) + \phi_2(\omega - \omega_o)^2 + \phi_3(\omega - \omega_o)^3 + \ldots$$

Ti:sapphire laser amplifier

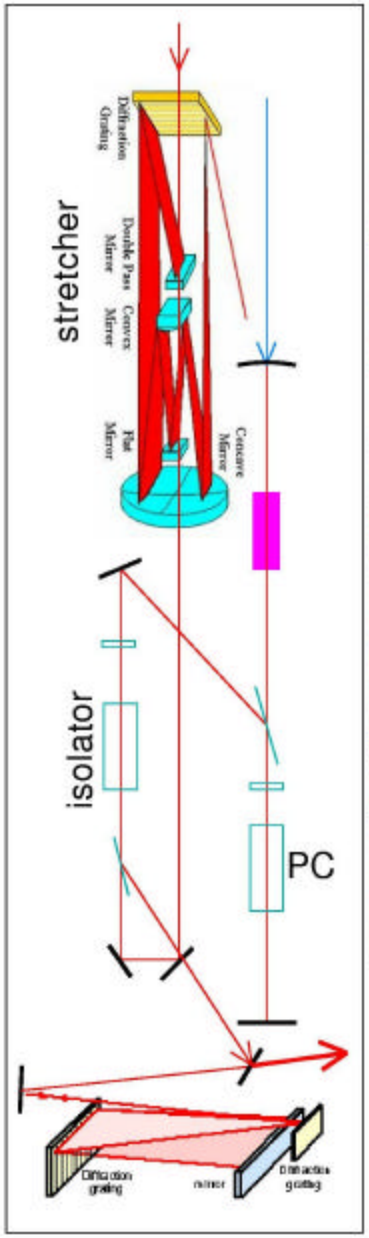

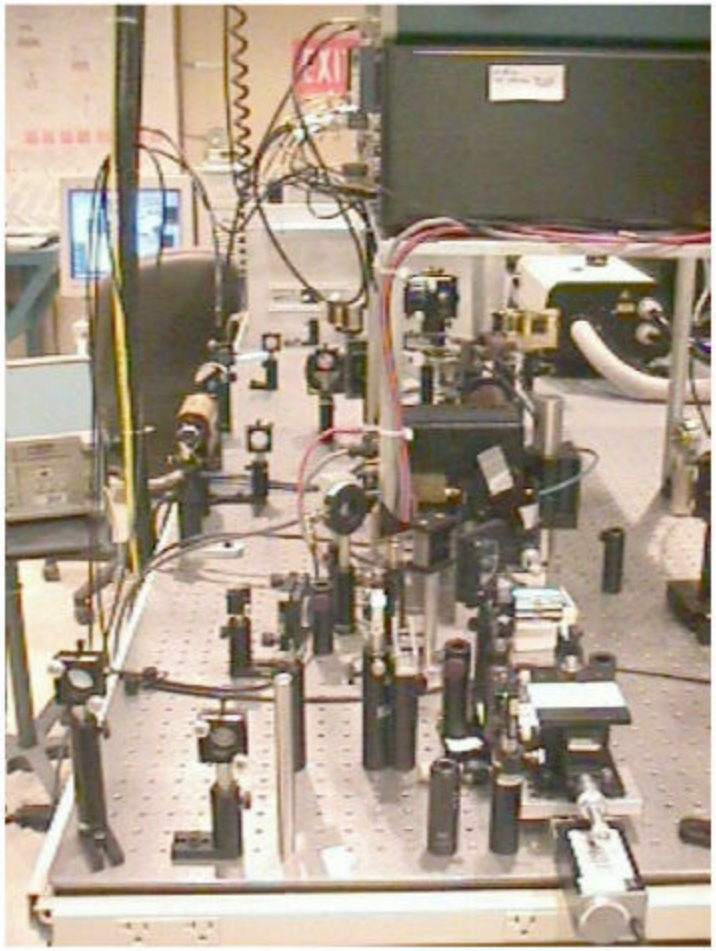

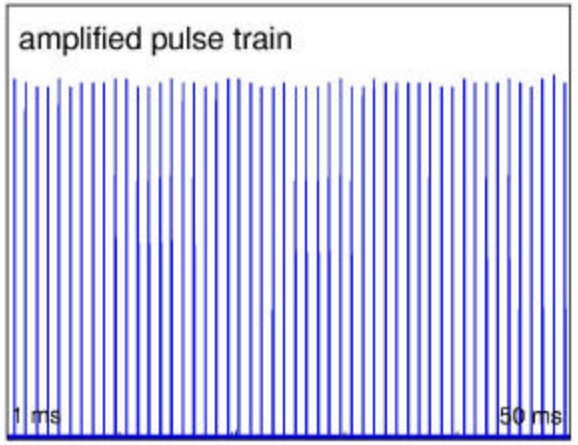

1 kHz repetition rate

200 fs

800 nm (1.55 eV)

0.8 mJ/pulse (~10^{15} photons)

4 GW/pulse

4×10^{17} Watts/cm^2

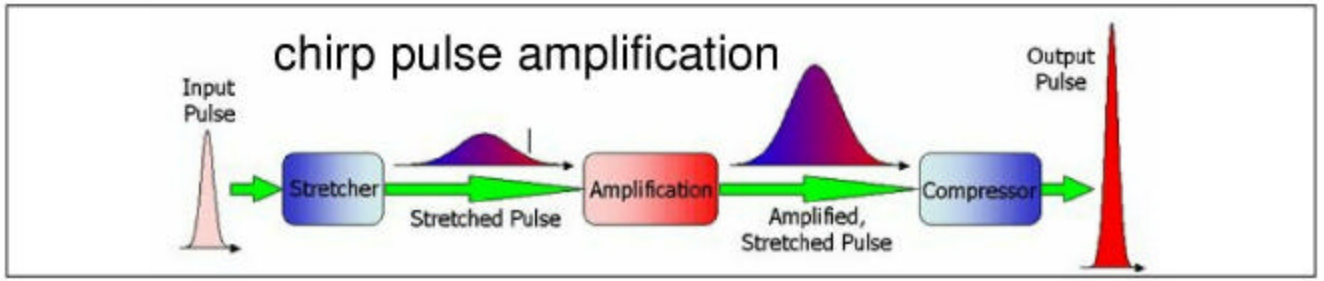

Pulse stretcher

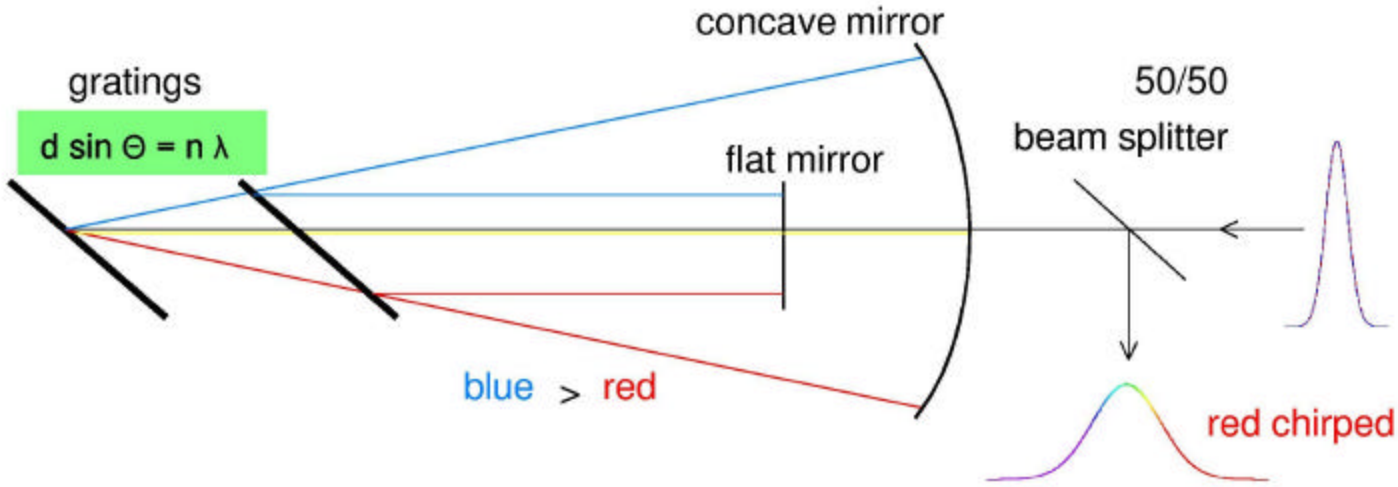

Grating compressor

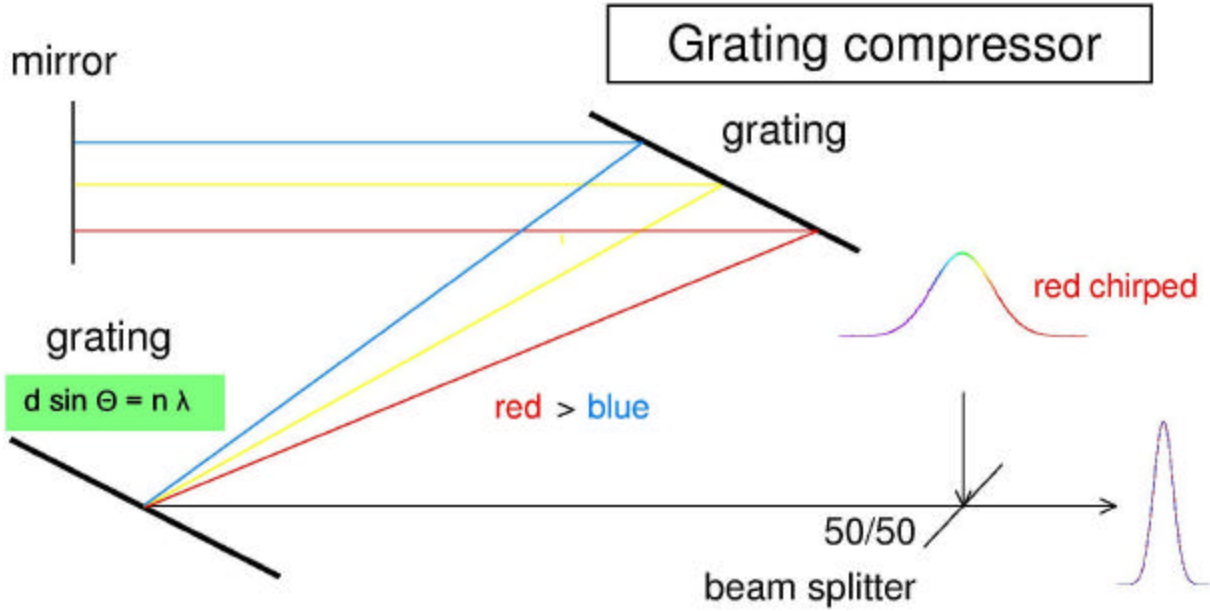

Group velocity dispersion (GVD) - linear effect

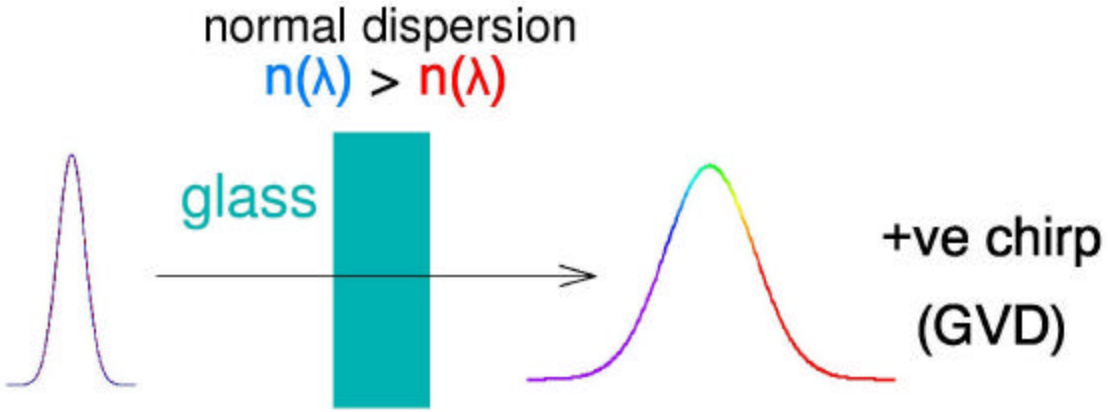

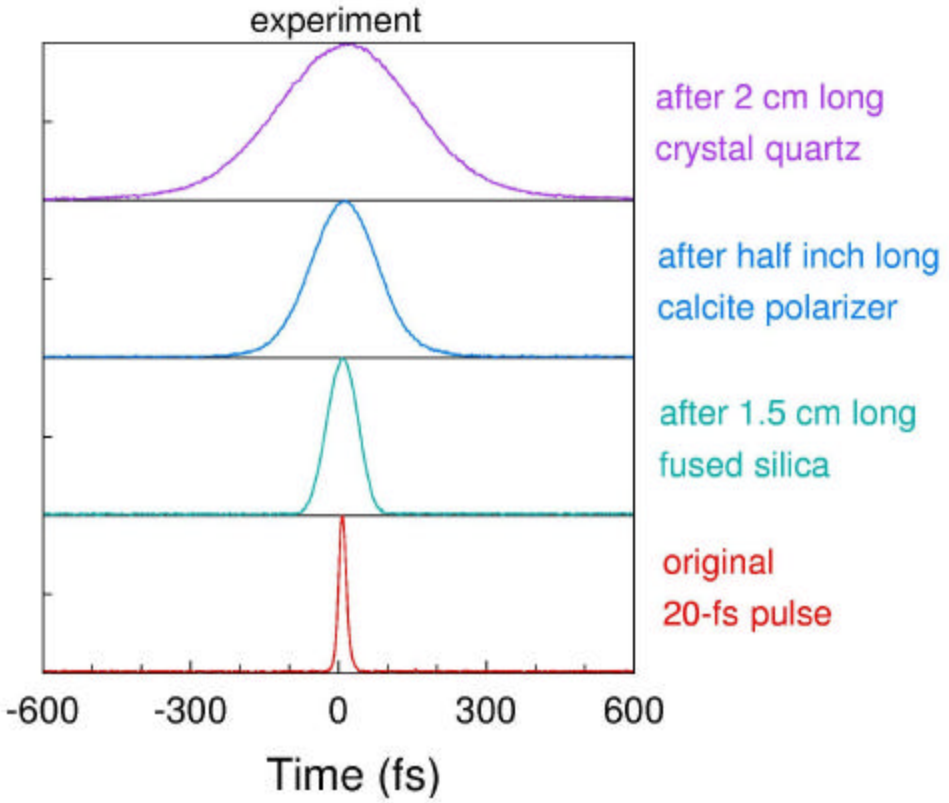

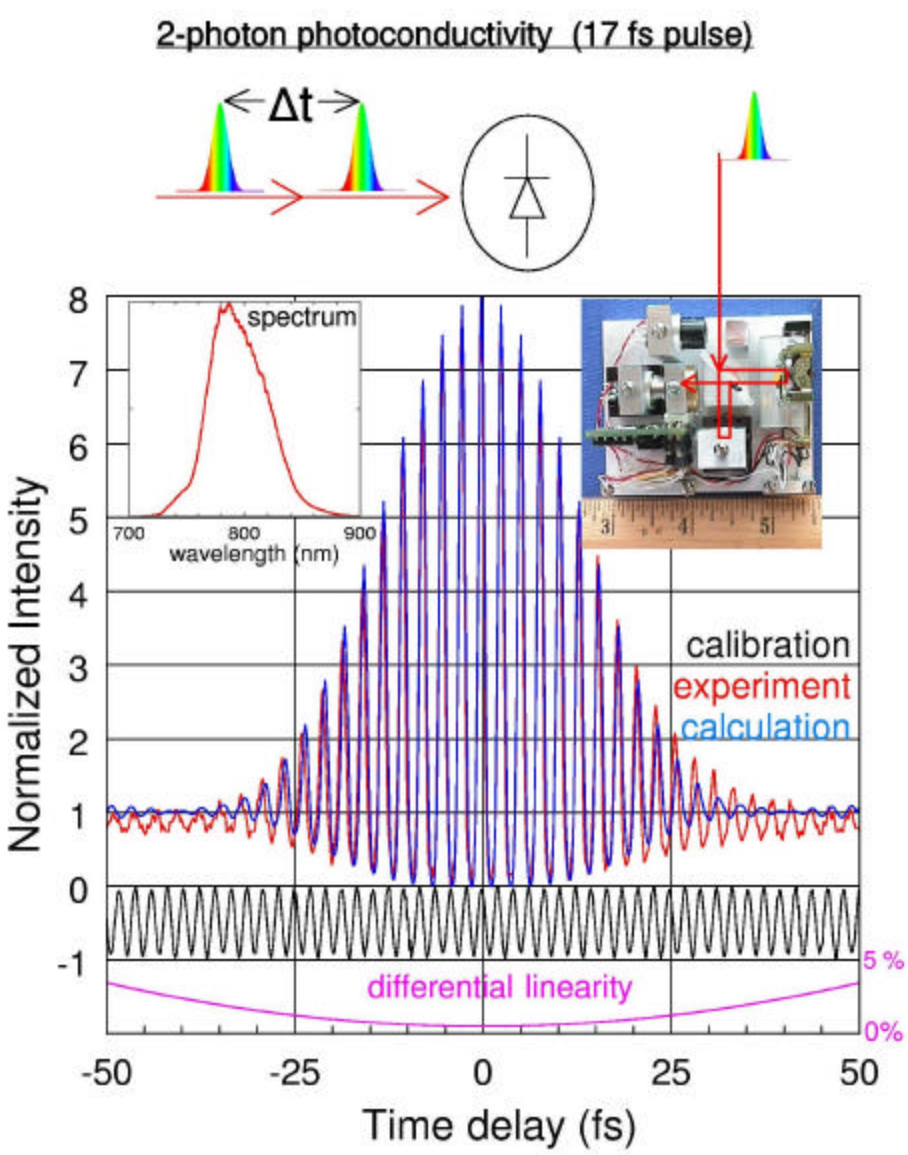
2-photon photoconductivity (17 fs pulse)
Δt
spectrum
700
800
900
wavelength (nm)
calibration
experiment
calculation
differential linearity
5 %
0%
Normalized Intensity
-50
-25
0
25
50
Time delay (fs)

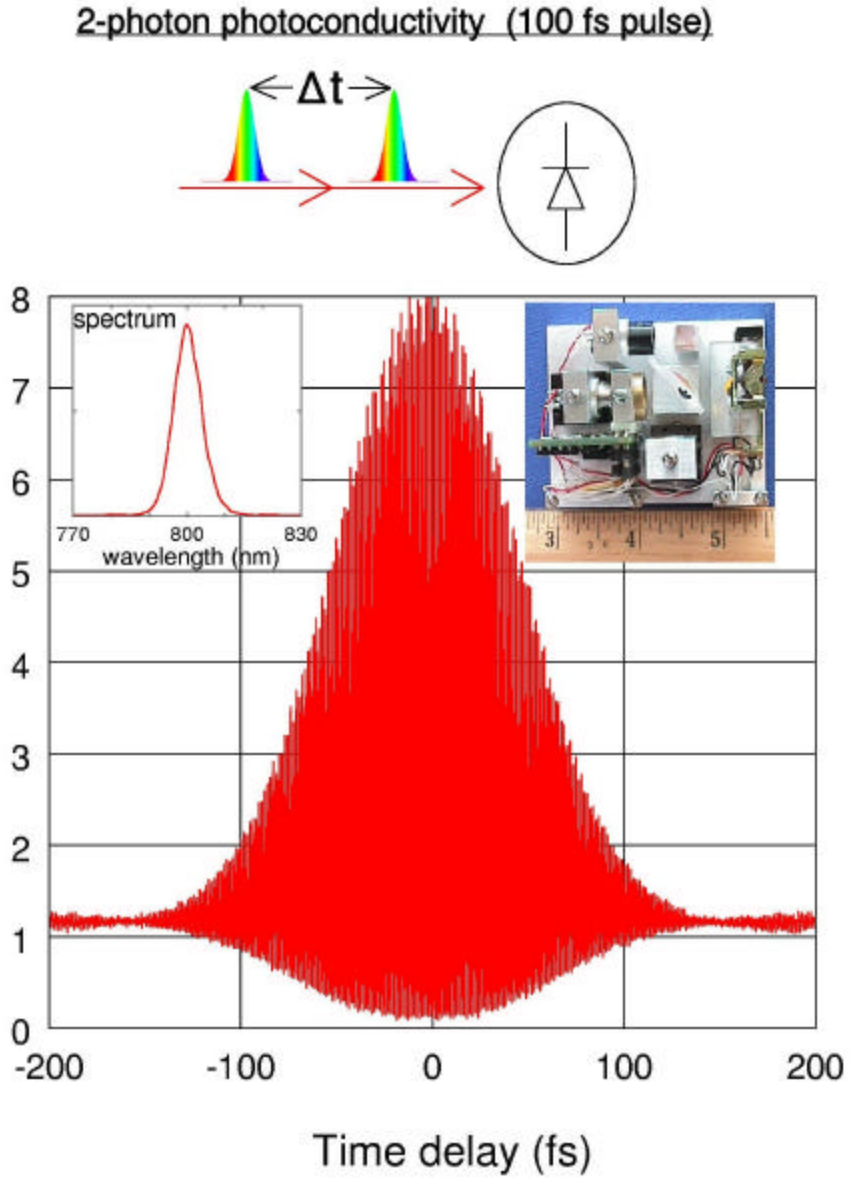
2-photon photoconductivity (100 fs pulse)
Δt
spectrum
770
800
830
wavelength (nm)
-200
-100
0
100
200
Time delay (fs)

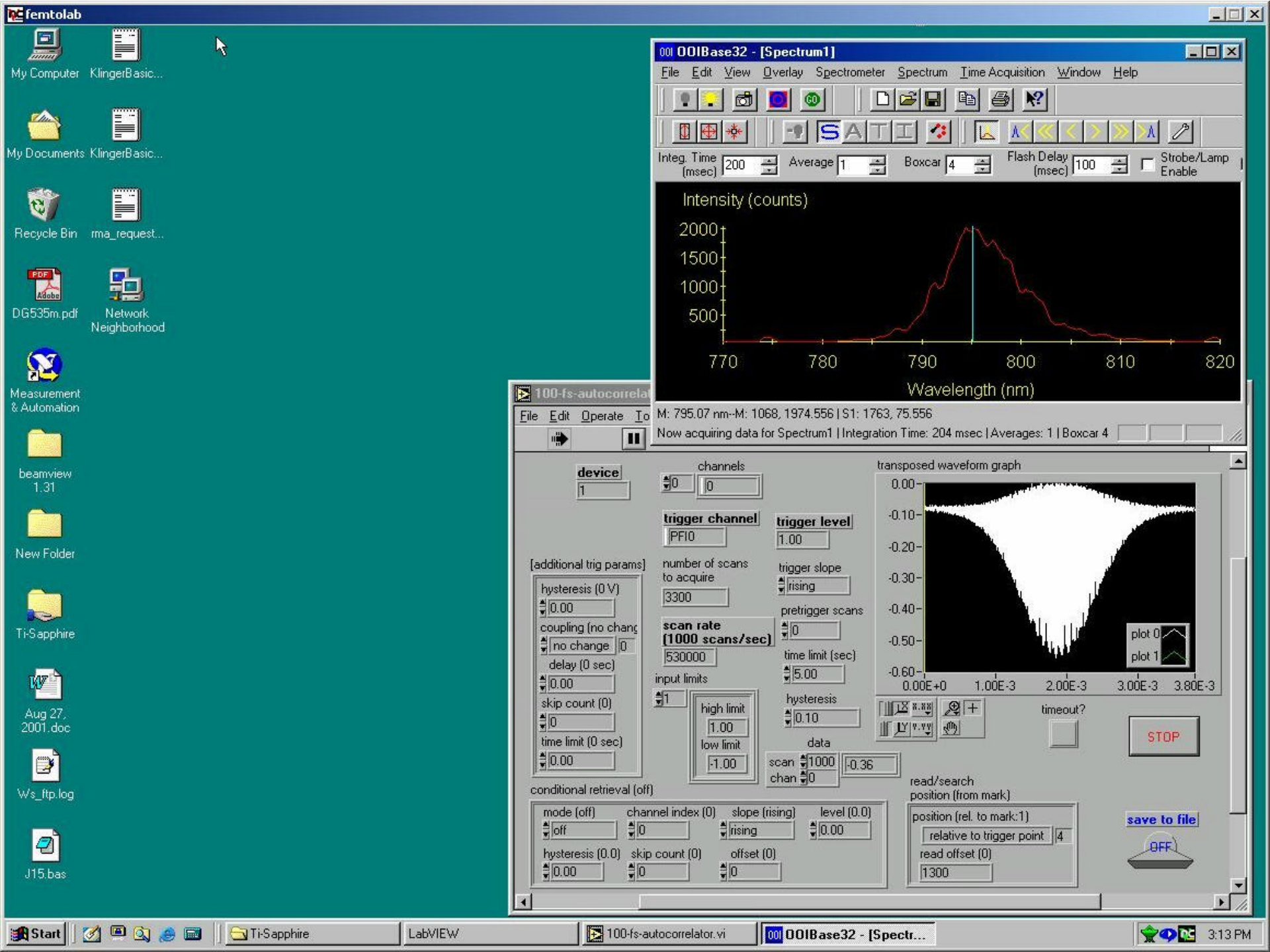
femtolab
My Computer
KlingerBasic...
My Documents
KlingerBasic...
Recycle Bin
rma_request...
DG535m.pdf
Network Neighborhood
Measurement & Automation
beamview 1.31
New Folder
Ti-Sapphire
Aug 27, 2001.doc
Ws_ftp.log
J15.bas
OOIBase32 - [Spectrum1]
File Edit View Overlay Spectrometer Spectrum Time Acquisition Window Help
Integ. Time (msec) 200
Average 1
Boxcar 4
Flash Delay (msec) 100
Strobe/Lamp Enable
Intensity (counts)
2000
1500
1000
500
770
780
790
800
810
820
Wavelength (nm)
M: 795.07 nm--M: 1068, 1974.556 | S1: 1763, 75.556
Now acquiring data for Spectrum1 | Integration Time: 204 msec | Averages: 1 | Boxcar 4
100-fs-autocorrela
File Edit Operate To
device
1
channels
0
0
trigger channel
PFI0
trigger level
1.00
[additional trig params]
hysteresis (0 V)
0.00
coupling (no chang
no change
0
delay (0 sec)
0.00
skip count (0)
0
time limit (0 sec)
0.00
number of scans to acquire
3300
trigger slope
rising
pretrigger scans
0
scan rate (1000 scans/sec)
530000
time limit (sec)
5.00
input limits
1
high limit
1.00
low limit
-1.00
hysteresis
0.10
data
scan 1000
chan 0
-0.36
transposed waveform graph
0.00
-0.10
-0.20
-0.30
-0.40
-0.50
-0.60
0.00E+0
1.00E-3
2.00E-3
3.00E-3
3.80E-3
plot 0
plot 1
timeout?
STOP
conditional retrieval (off)
mode (off)
off
channel index (0)
0
slope (rising)
rising
level (0.0)
0.00
hysteresis (0.0)
0.00
skip count (0)
0
offset (0)
0
read/search position (from mark)
position (rel. to mark:1)
relative to trigger point
4
read offset (0)
1300
save to file
OFF
Start
Ti-Sapphire
LabVIEW
100-fs-autocorrelator.vi
OOIBase32 - [Spectr...
3:13 PM

FROG - frequency-resolved optical gating - Third-harmonic generation

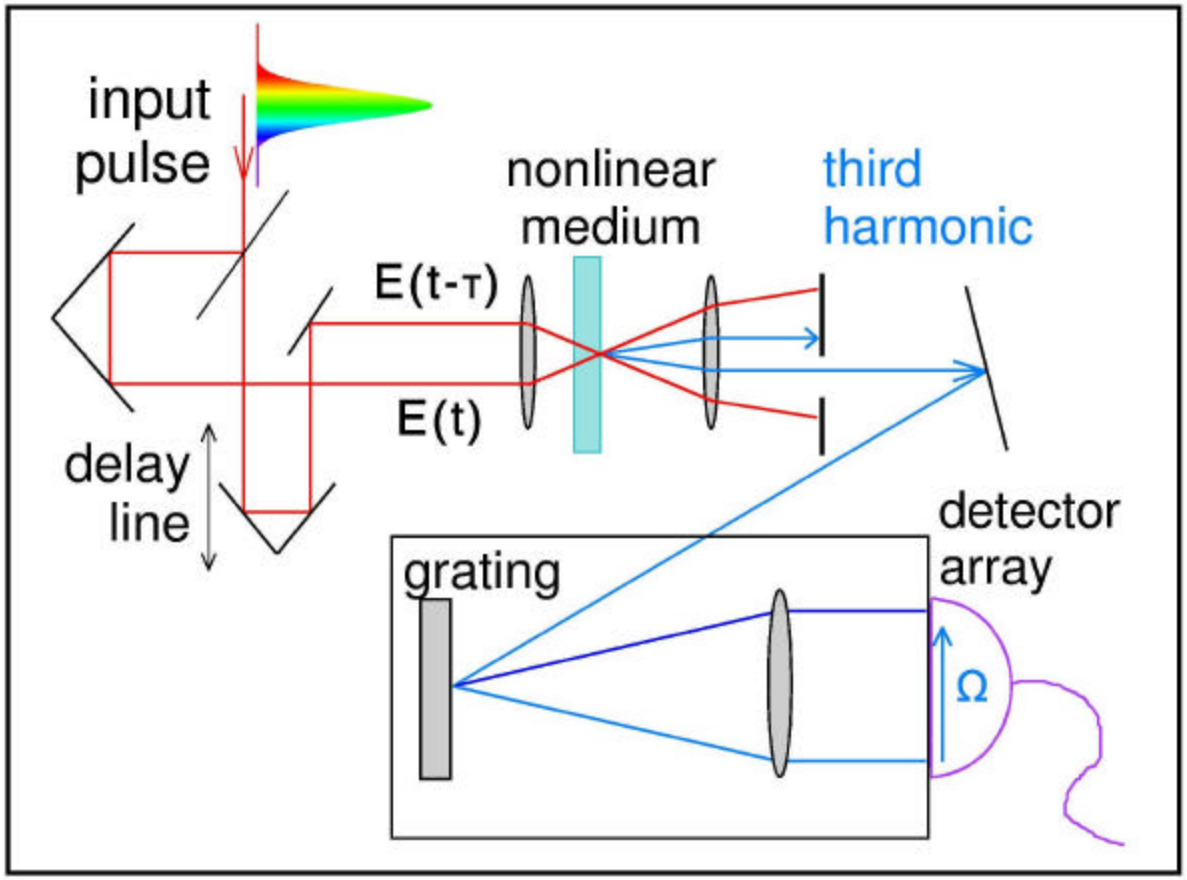

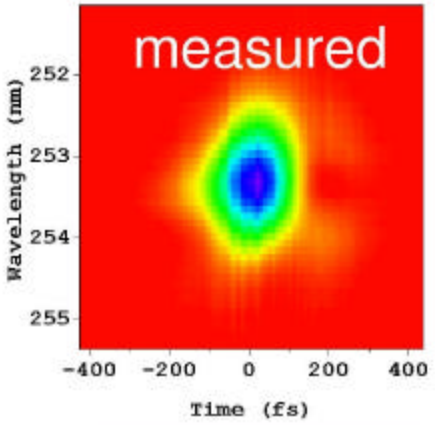

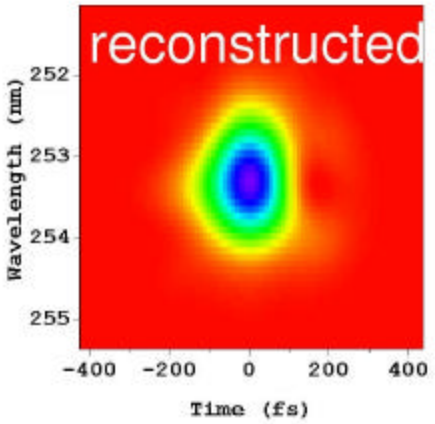

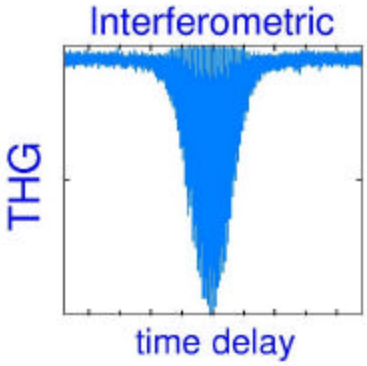

$$\mathbb{E} = E(t)e^{i\phi(t)}$$

$$\omega = \omega(t)e^{i\theta(t)}$$

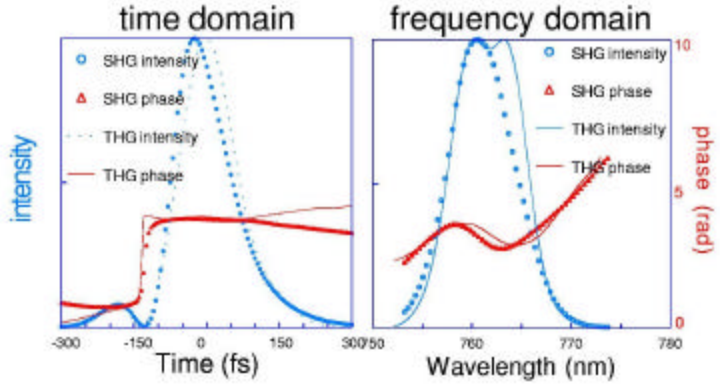

heat diffusion time ~ns-μs duration

electron-phonon relaxation time ~ps

nonequilibrium temperatures

$$C_e(T_e)\frac{\partial T_e}{\partial t} = \kappa\Delta^2 T_e - G(T_e - T_l) + P_o(r,t)$$

$$C_l\frac{\partial T_l}{\partial t} = G(T_e - T_l)$$

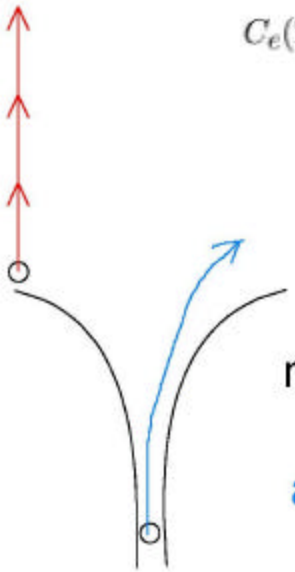

metals and opaque materials

avalanche ionization

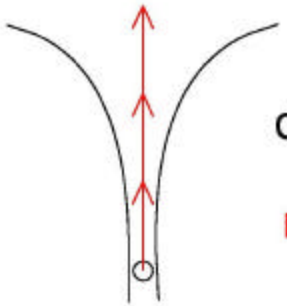

dielectric materials

multiphoton absorption

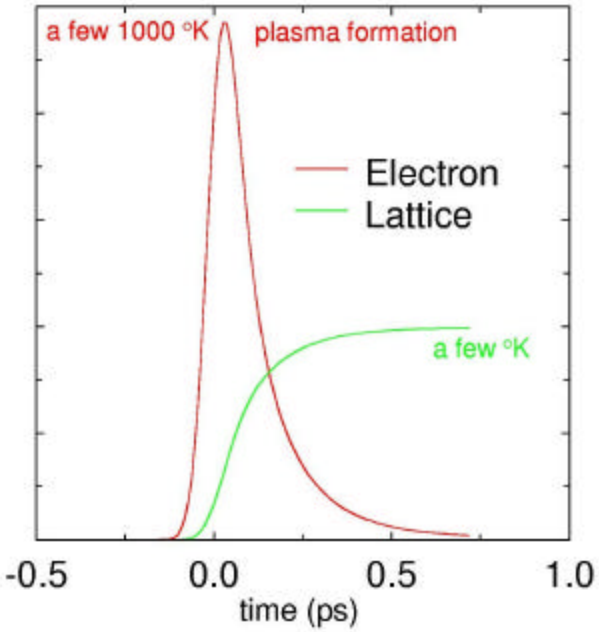

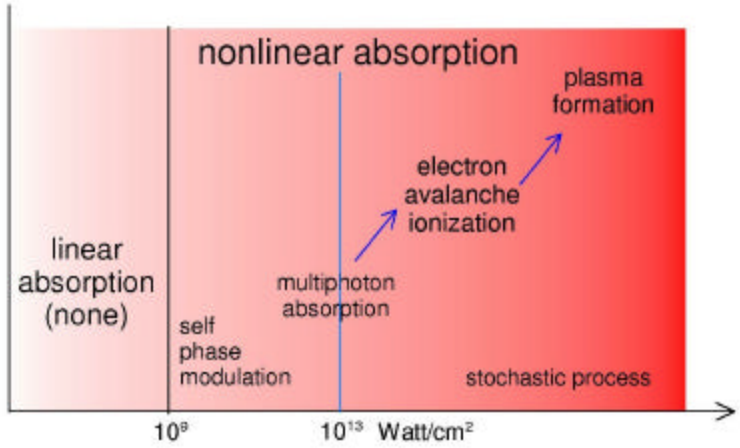

- Animation of long pulses versus short pulses

Animation Index File (click here to open)

A channel machined in 1 mm thick INVAR, Nickel/Iron alloy under the same experimental conditions as the long pulse channel in Figure 4.1, but with ultrafast pulses. This channel was machined with 200 femtosecond pulses, 0.5 mJ energy per pulse. It is quite obvious that the channel machined with femtosecond pulses is cleaner than the sample machined with nanosecond pulses (place link to figure 4.1). Note also the absence of a recast layer. It is also clear that the machining process was more efficient – the channel is larger. The edges are straighter. Overall the quality of the micromachining is much higher.

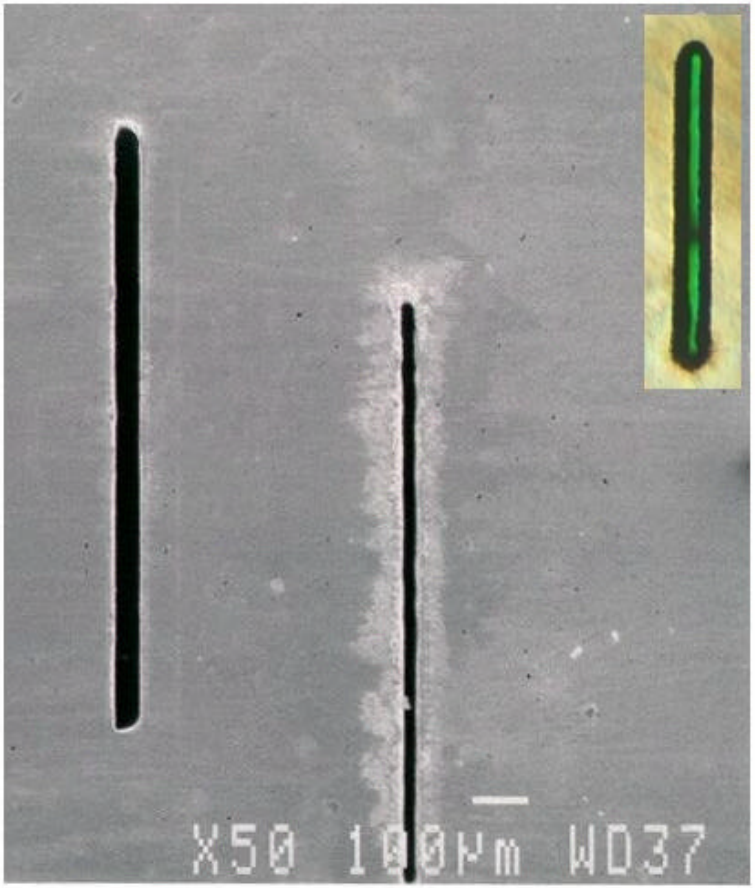

Source: Clark-MXR, Inc.

Figure 6.1: Channel machined in INVAR with ultrafast laser.

Process of Dielectric breakdown

- excitation of electron in conduction band by multi-photon (or impact) ionization
- heating of conduction band by free electron to form a critical density electron plasma
- continue absorption of laser energy by plasma
- plasma expands as a highly energetic gas
- heat diffusion is "frozen" during laser interaction, minimum energy is deposited to the lattice.
- process is precise and reproducible - a controlled damage

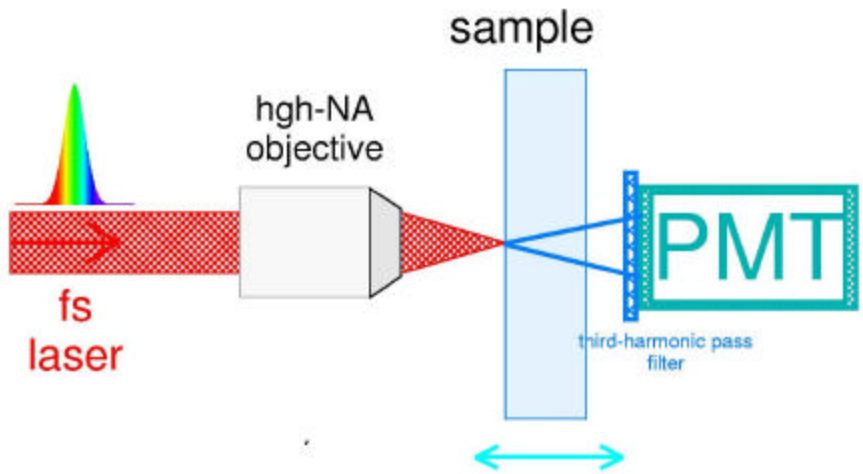
sample
hgh-NA
objective
fs
laser
PMT
third-harmonic pass
filter

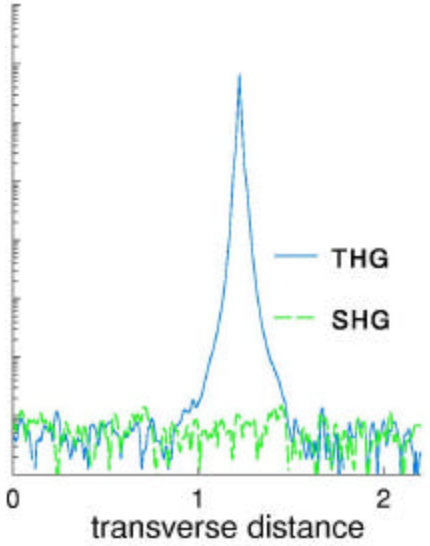
THG
SHG
0
1
2
transverse distance

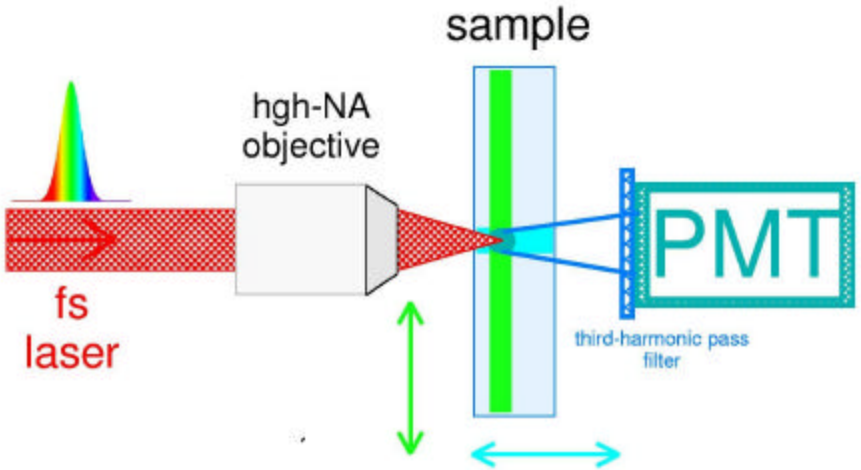
sample
hgh-NA
objective
fs
laser
PMT
third-harmonic pass
filter

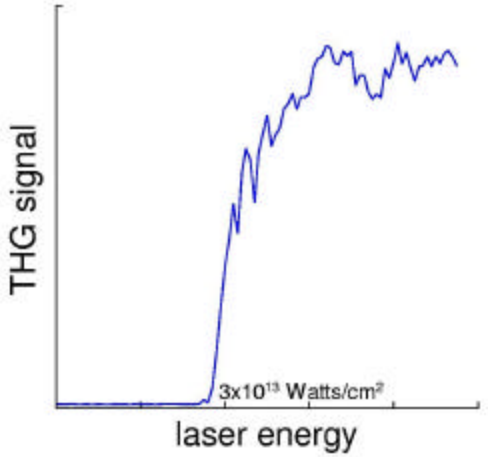
THG signal
3x10^13 Watts/cm^2
laser energy

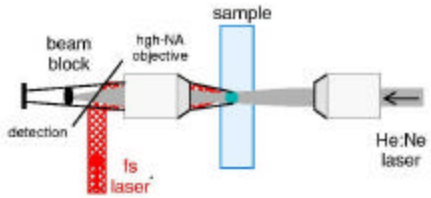
sample
beam
block
hgh-NA
objective
detection
fs
laser
He:Ne
laser

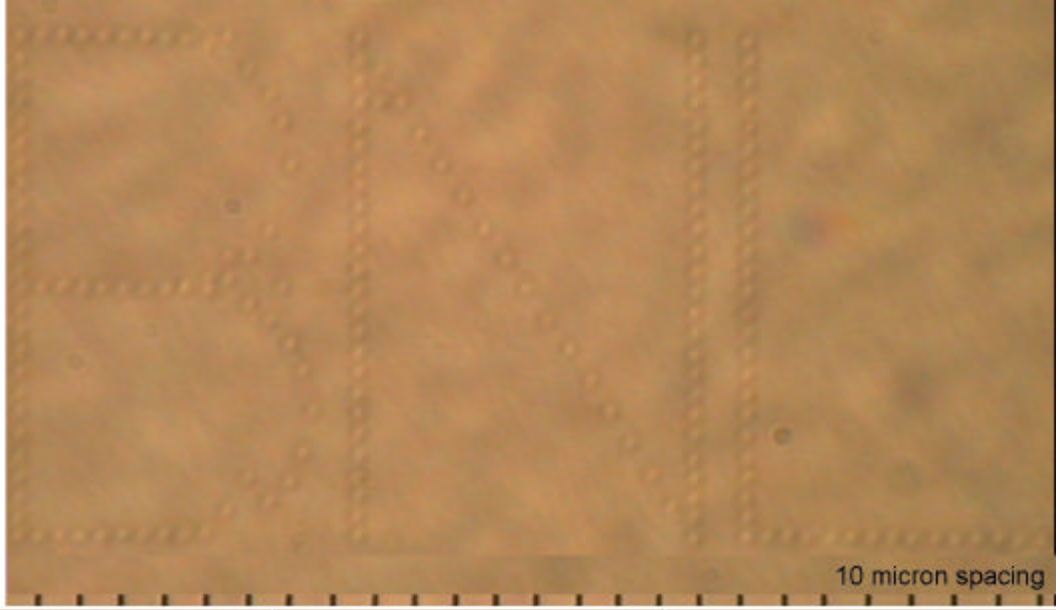
10 micron spacing

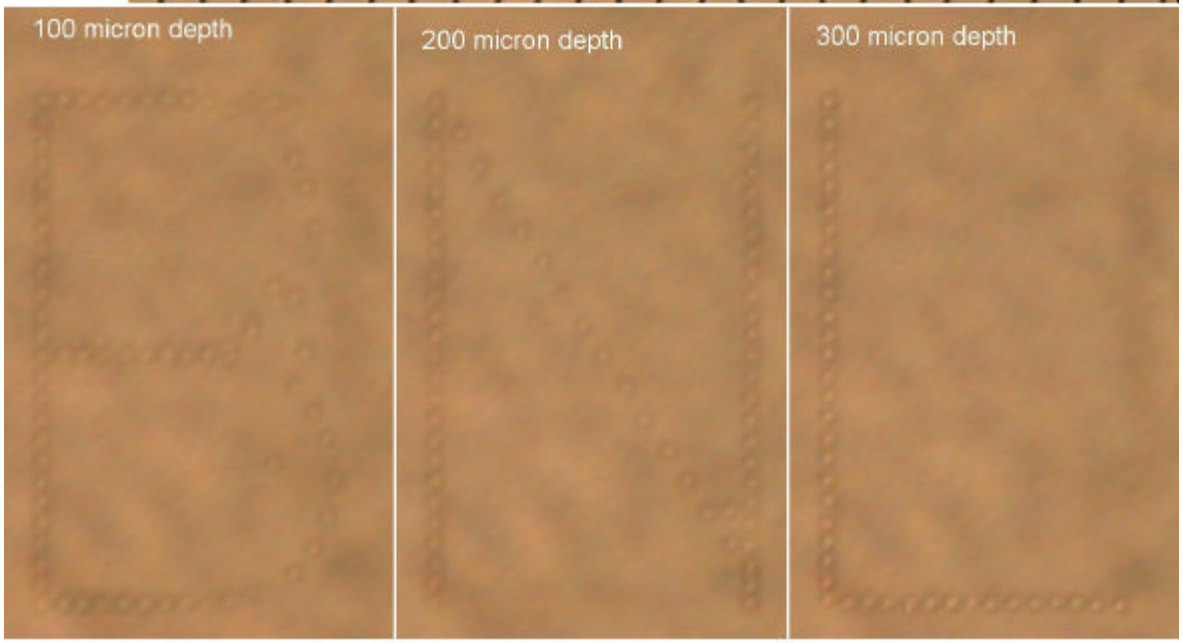
100 micron depth
200 micron depth
300 micron depth

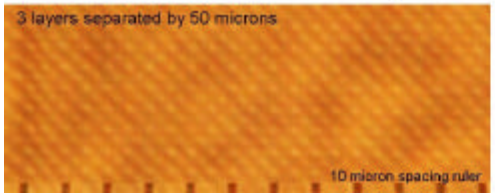
3 layers separated by 50 microns
10 micron spacing ruler

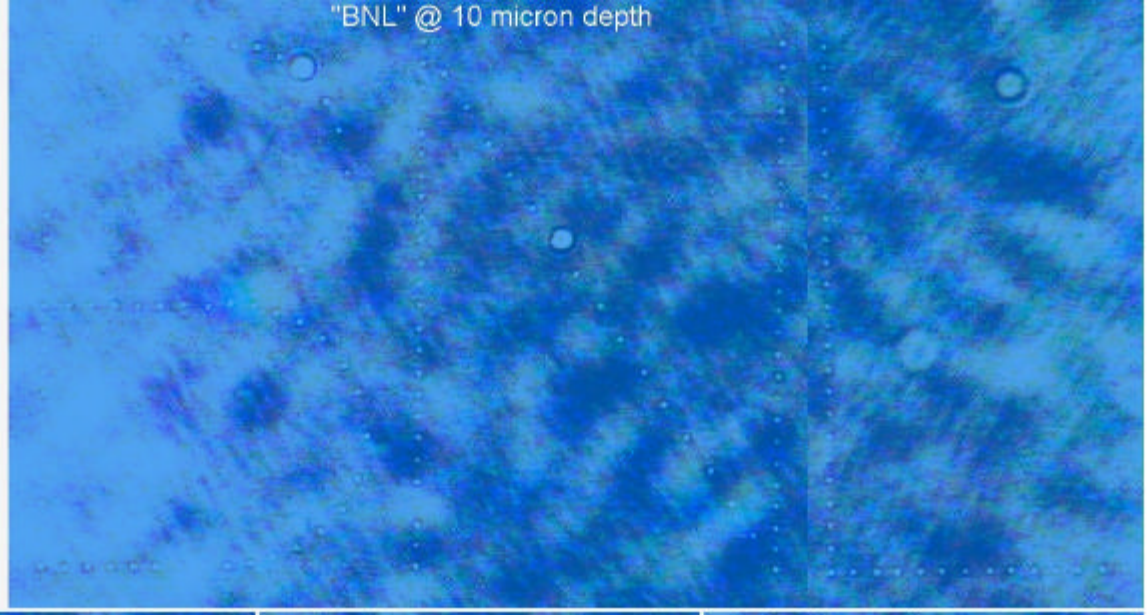

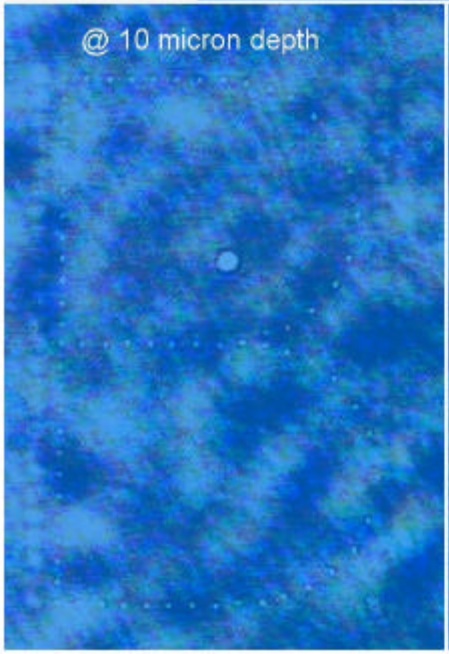

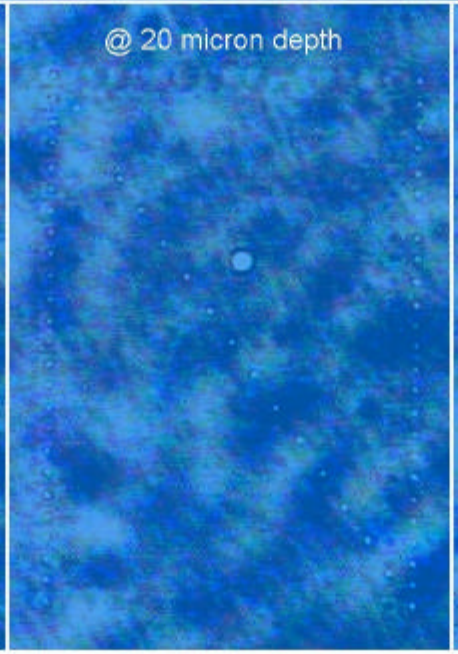

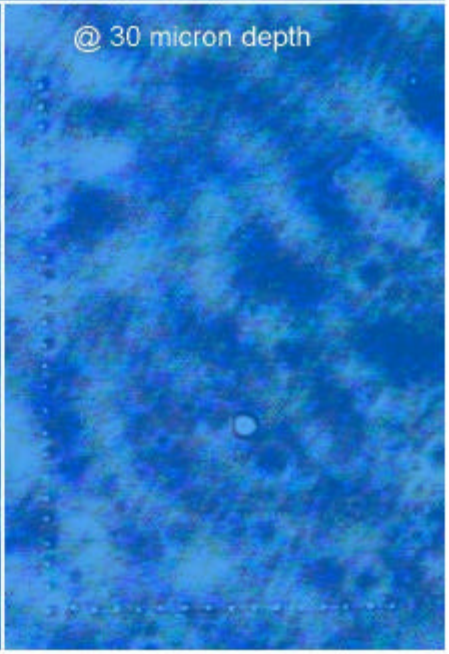

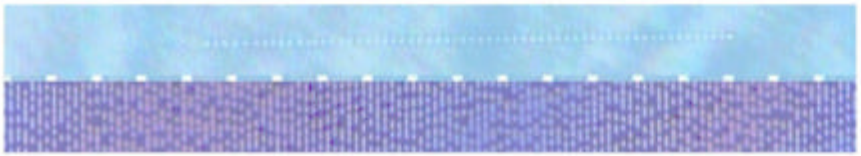

	650 MB CD	4.7 GB DVD	3-D dielectric
density	6.5 MB/cm^2	47 MB/cm^2	10^5 - 10^6 MB/cm^3
bit size	15 μm^2/bit	2 μm^2/bit	$1-10$ μm^3/bit

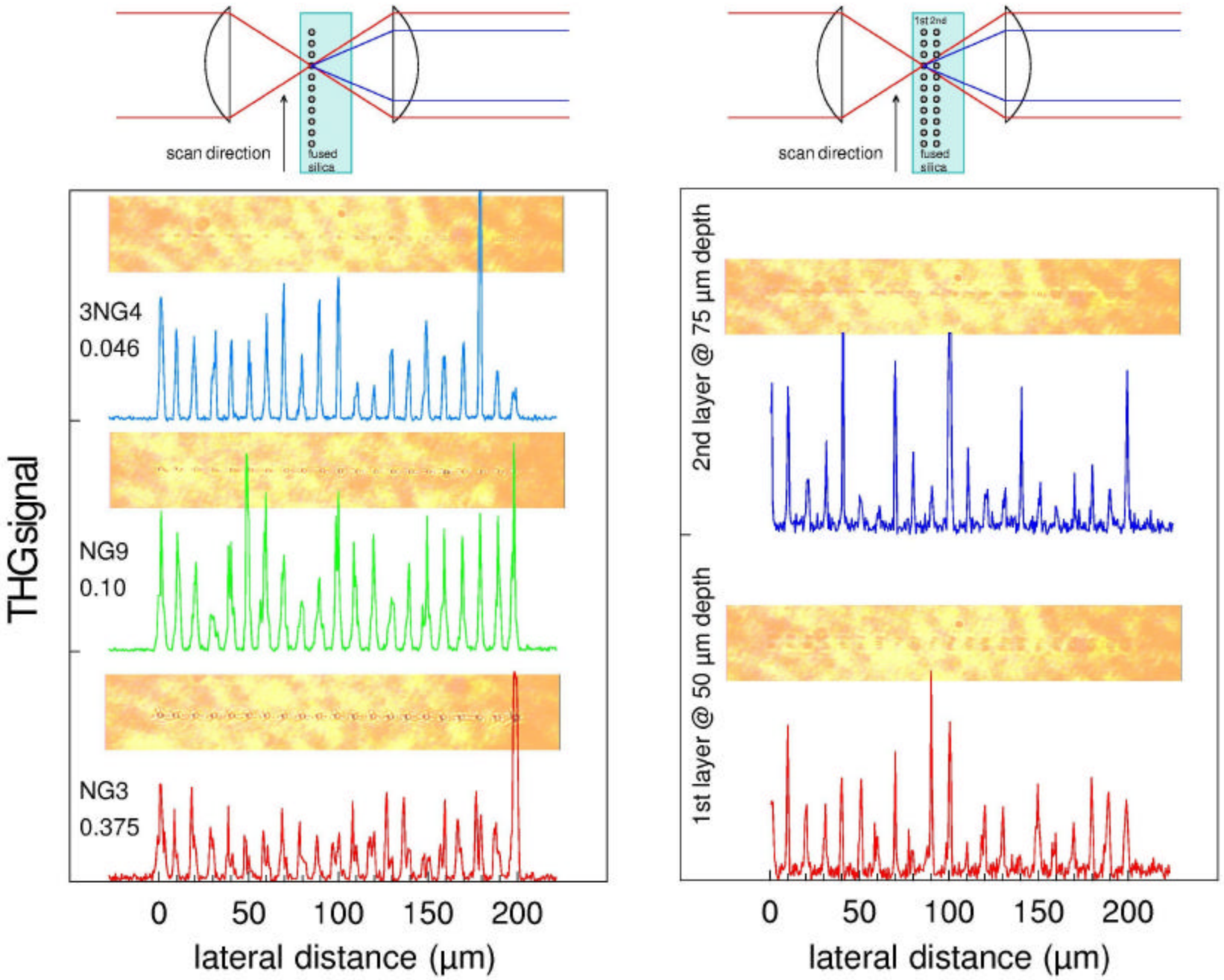
scan direction
fused silica
1st 2nd
scan direction
fused silica
THG signal
3NG4
0.046
NG9
0.10
NG3
0.375
2nd layer @ 75 µm depth
1st layer @ 50 µm depth
0
50
100
150
200
lateral distance (µm)
0
50
100
150
200
lateral distance (µm)

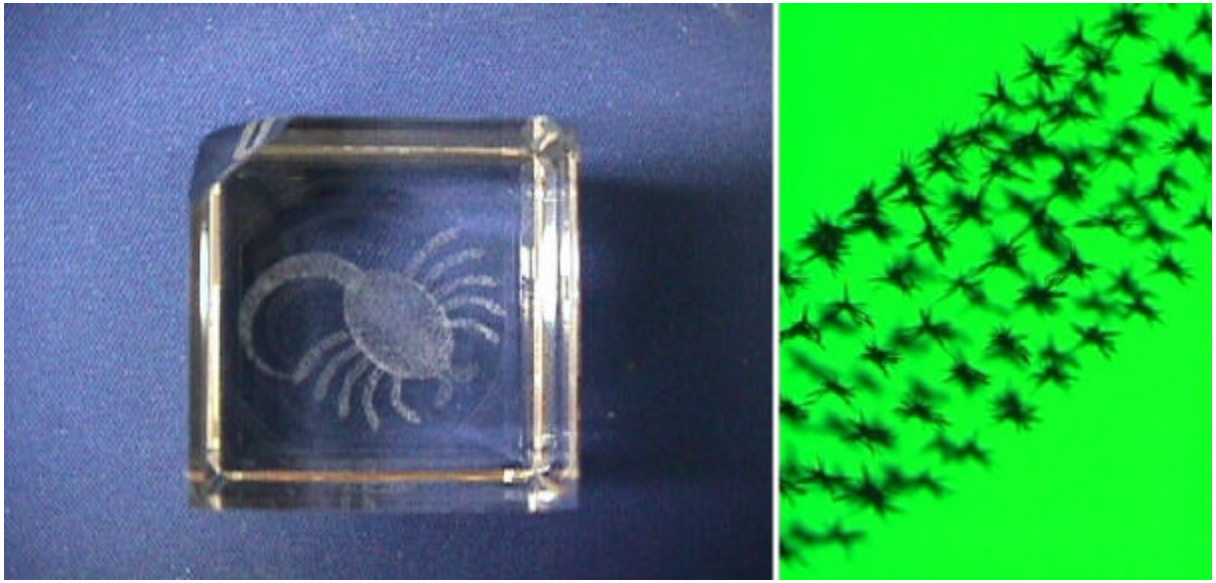

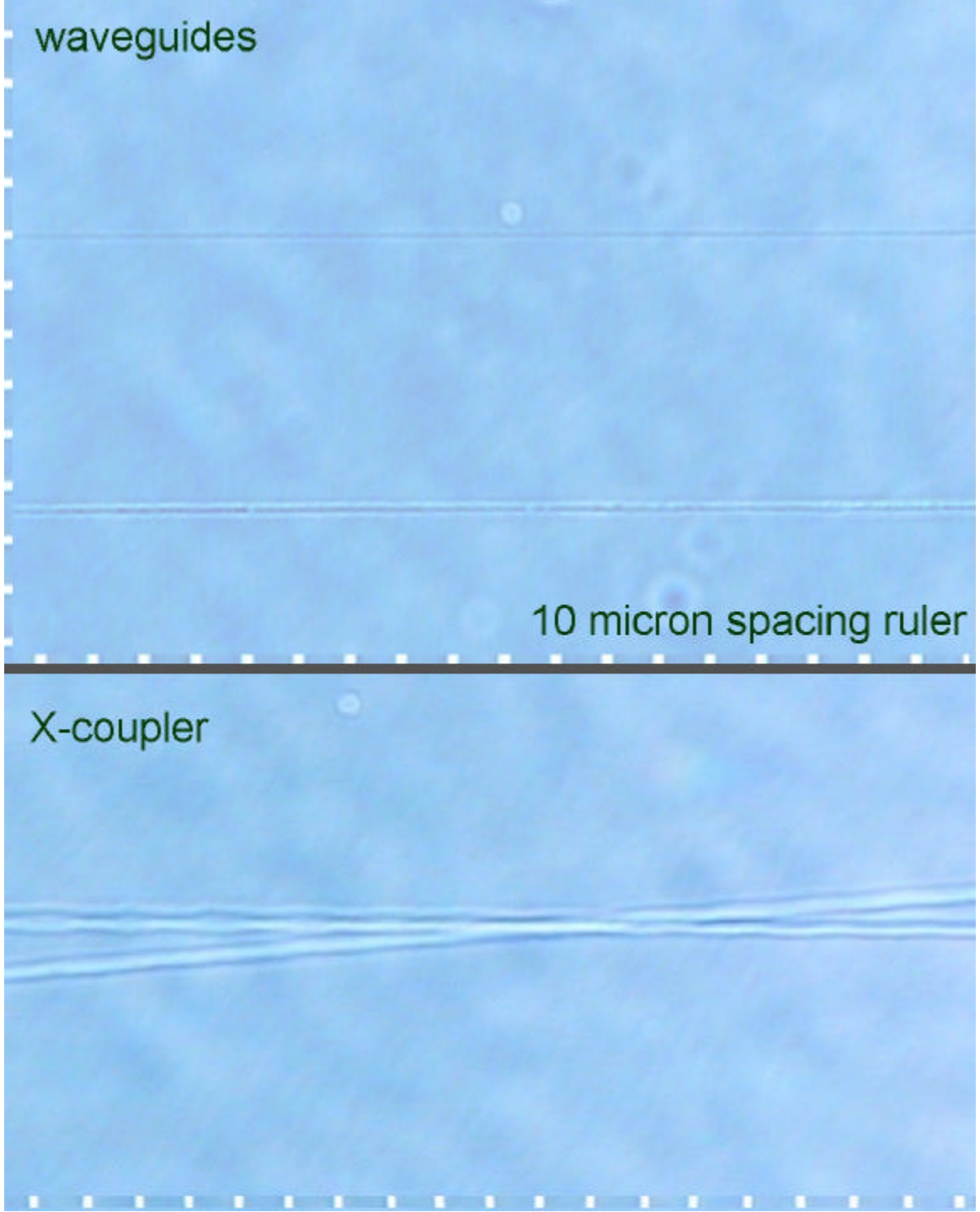
waveguides
10 micron spacing ruler
X-coupler

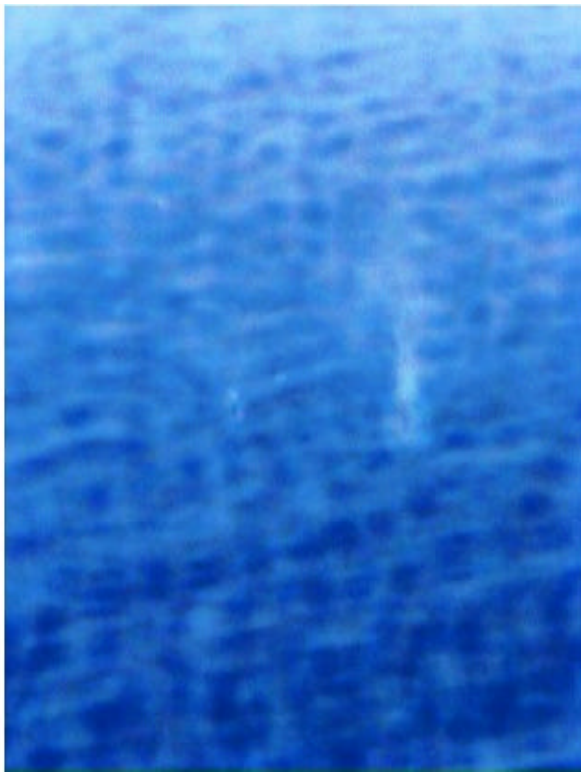

some laser machining parameters

pulse width	200 fs
spot size	1-2 μm diameter
power density	$\sim$ 8x10^{13} Watts/cm^2
energy density	$\sim$ 16 Joule/cm^2
energy/pulse	160 nanoJoule/pulse
# of pulses	$10^3 - 10^4$
Δn	$10^{-3} - 10^{-4}$

$$E_{th} = \text{power threshold} = \frac{I_{th}\tau\lambda^2}{\pi(NA)^2 + I_{th}\frac{\lambda}{P_{cr}}} = \sim 3\text{x}10^{13} \text{ Watts/cm}^2$$

P_{cr} = critical power for self focusing

I_{th} = optical breakdown threshold

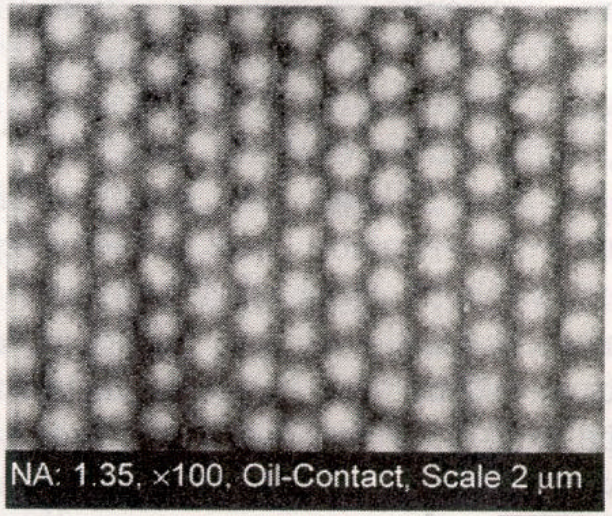

(b)

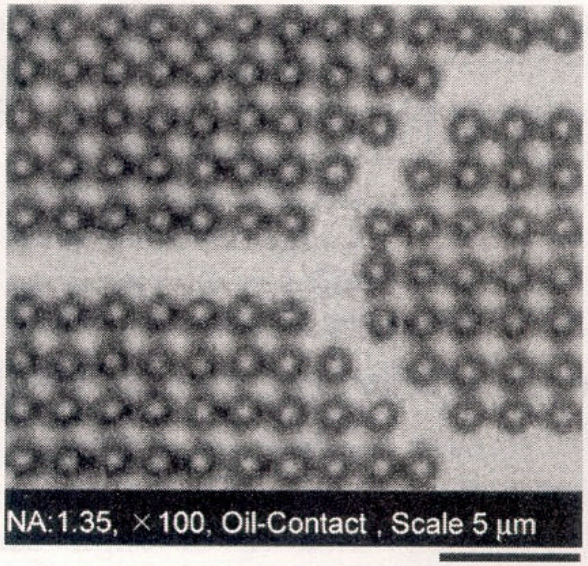

Fig. 1. (100) Plane of an *sc* photonic lattice in Ge-doped silica. The empty Y-shaped area consists of missing photonic atoms and functions as a microintegrated optical waveguide.

Sun, et. al., Optics Letters 26, 325 (2001)

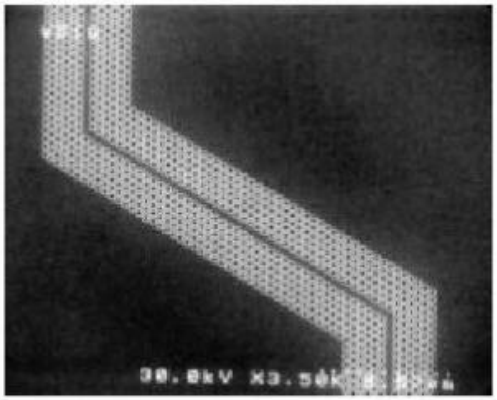

(a)

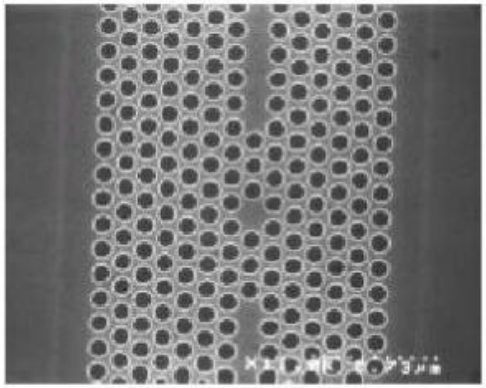

(b)

Fig. 8. (a) Waveguide with two 60° bends and 25 μm bend-to-bend spacing. (b) High-Q cavity filter formed by coupling single-defect cavity to the two waveguide sections.

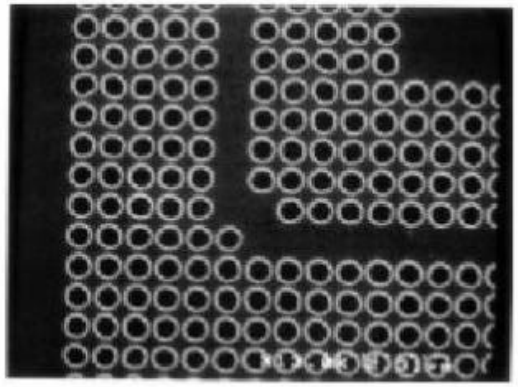

(a)

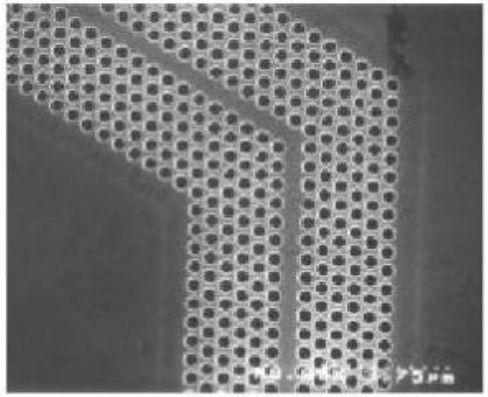

(b)

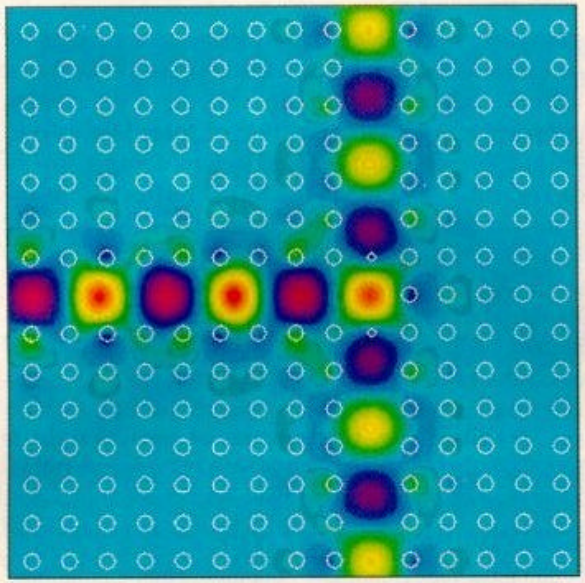

-1.00 0.00 1.00

Figure 2. Steady-state field distribution in a photonic crystal waveguide branch, at a frequency where nearly 100% transmission occurs. White circles indicate the positions of the dielectric cylinders. Plotted here is the amplitude of the electric field component that is parallel to the cylinders.

Fan and Joannopoulos, Optics and Pohtonic News, Oct. 2000

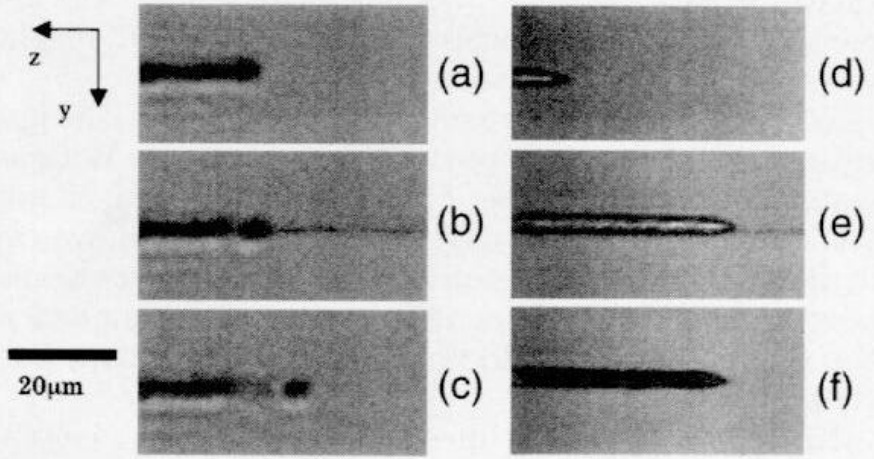

Fig. 2. Microdrilling of silica glass from its rear surface in air without and with an inflow of water into the hole. Incident energy, 1 μJ per pulse. (a)–(c) Drilling without an inflow of water; (d), (e) drilling with an inflow of water. (f) Image of (e) after the water has receded.

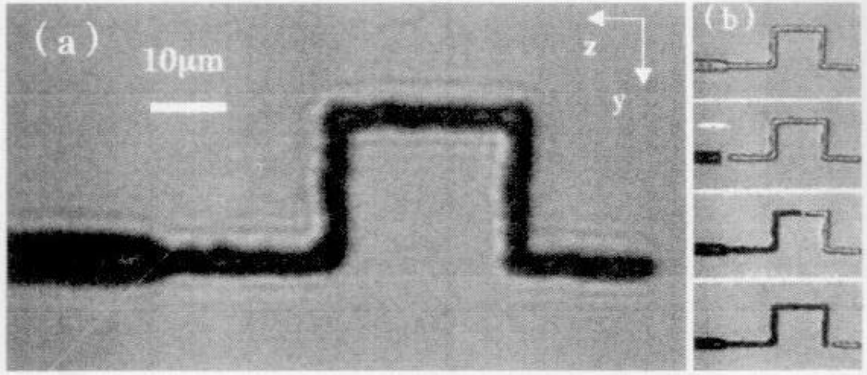

Fig. 4. Square-wave shaped hole drilled by movement of the sample in different directions. (a) The finished hole with diameters of ~7 μm (pulse energy, ~4 μJ) and ~4 μm (pulse energy, ~1 μJ). (b) Video clips of the drying process of the refilled hole.

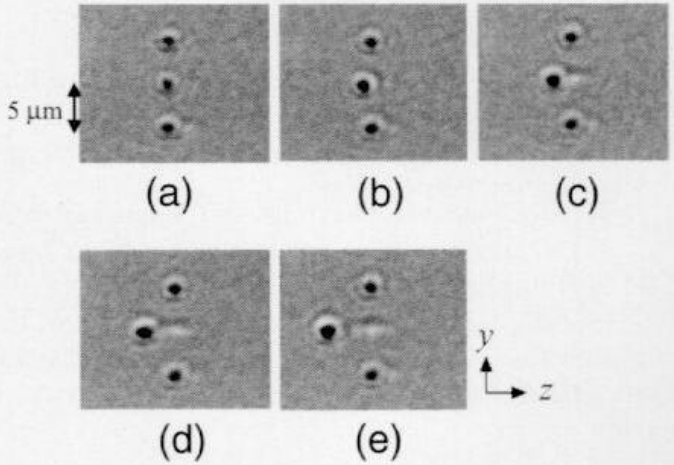

Fig. 2. (a)–(d) Side views of optical seizing and movement of a void. (e) Central void is moved toward the input plane by 5 μm.

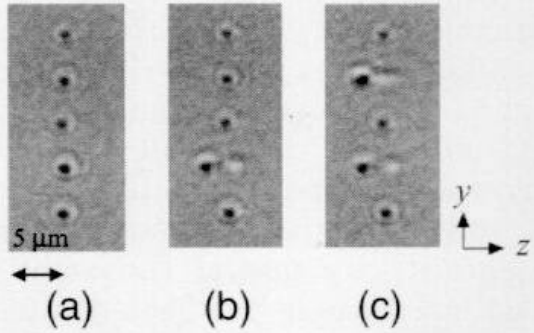

Fig. 3. Optical movement of arbitrary voids: (a) creation of voids, (b) movement of the fourth void, (c) movement of the second void.

Large-scale optical integration - in 3-D

- high-density optical memory devices 
- waveguides - singlemode, multimode, hollow channels 
- directional couplers, X-coupler 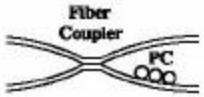

- circulators, fiber gratings, modulators 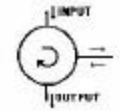

- photonic 2-D and 3-D crystals 
- holey waveguides 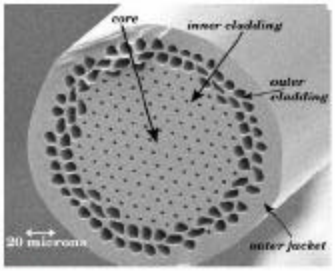

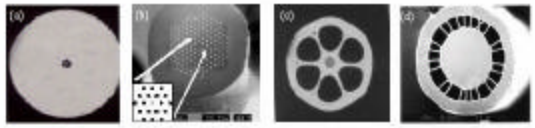

Conclusions

- Potential to create large-scale optical integration in 3-D
- Re-writable optical components may be possible
- High precision micromachining of virtually all optical materials
- Potential to produce sub-micron, or nano-meter features